Journal of Cellular Biochemistry 96:599–610 (2005)

Differential Localization of Acetylcholinesterase in Neuronal and Non-Neuronal Cells

Matthew D. Thullbery,[1,3] Holly D. Cox,[2,3] Travis Schule,[3] Charles M. Thompson,[1,2,3] and Kathleen M. George[1,2,3]*

[1]Center for Environmental Health Sciences, The University of Montana, Missoula, Montana
[2]Center for Structural and Functional Neuroscience, The University of Montana, Missoula, Montana
[3]Department of Biomedical and Pharmaceutical Sciences, The University of Montana, Missoula, Montana

Abstract Acetylcholinesterase (AChE) expression is regulated in cell types at the transcriptional and translational levels. In this study, we characterized and compared AChE catalytic activity, mRNA, protein expression, and protein localization in a variety of neuronal (SH-SY5Y neuroblastoma and primary cerebellar granule neurons (CGN)) and non-neuronal (LLC-MK2, HeLa, THP-1, and primary astrocytes) cell types. All cell lines expressed AChE catalytic activity; however the levels of AChE-specific activity were higher in neuronal cells than in the non-neuronal cell types. CGN expressed significantly more AChE activity than SH-SY5Y cells. All cell lines analyzed expressed AChE protein at equivalent levels, as well as mRNA splice variants. Localization of AChE was characterized by immunofluorescence and confocal microscopy. SH-SY5Y, CGN, and nerve-growth factor-differentiated PC-12 cells exhibited a pattern of AChE localization characterized as diffuse in the cytoplasm and punctate staining along neurites and on the plasma membrane. The localization in HeLa, LLC-MK2, fibroblasts, and undifferentiated PC-12 cells was significantly different than in neuronal cells—AChE was intensely localized in the perinuclear region, without staining near or on the plasma membrane. Based on the evidence presented here, we hypothesize that the presence of AChE protein doesn't correlate with catalytic activity, and the diffuse cytoplasmic and plasma membrane localization of AChE is a property of neuronal cell types. J. Cell. Biochem. 96: 599–610, 2005. © 2005 Wiley-Liss, Inc.

Key words: acetylcholinesterase; confocal microscopy; cerebellar granule neuron; neuroblastoma; SH-SY5Y; HeLa; PC-12

Acetylcholinesterase (AChE) belongs to the serine hydrolase family that contains the α/β hydrolase fold as a common structural element [Ollis et al., 1992]. The catalytic active site of AChE is made up of a precise arrangement of active site functional groups that catalyze the hydrolytic breakdown of esters that bear quaternary ammonium groups. The biological importance of AChE-catalyzed hydrolysis is manifested in the rapid termination of the neuronal impulse that occurs when acetylcholine (ACh) is released into the synaptic cleft. AChE rapidly hydrolyzes ACh into acetic acid and choline at extremely fast turnover rates [Taylor and Radic, 1994].

Although the primary role of AChE is hydrolysis of ACh, alternative functions for AChE have been demonstrated in neuronal and hematopoietic cells that are independent of catalytic activity and have been reviewed extensively [Grisaru et al., 1999; Soreq and Seidman, 2001]. AChE is involved in cell adhesion, proliferation, and neurite outgrowth in diverse types of neurons, including non-cholinergic neurons [Karpel et al., 1996; Koenigsberger et al., 1997; Day and Greenfield, 2002; Whyte and Greenfield, 2003; Johnson and Moore, 2004]. In the hematopoietic system, AChE inhibits proliferation of multipotent stem cells and regulates apoptosis [Soreq et al., 1994]. Other functions attributed to AChE include promotion of amyloid fiber assembly and amidase activities

Grant sponsor: Department of the Army; Grant number: DAMD17-01-0795; Grant sponsor: National Science Foundation; Grant numbers: MCB9808372, EPS0091995.

*Correspondence to: Kathleen M. George, PhD, Department of Biomedical and Pharmaceutical Sciences, The University of Montana, Missoula, MT 59812.
E-mail: kgeorge@spahs.umt.edu

Received 10 March 2005; Accepted 26 April 2005
DOI 10.1002/jcb.20530

[Checler et al., 1994; Inestrosa et al., 1996; Boopathy and Layer, 2004]. AChE expression is not restricted to cholinergic neurons and hematopoietic cells. AChE has been shown to be expressed in osteoblasts, vascular endothelial cells, leukocytes, and to be induced in various cell lines undergoing apoptosis [Lan et al., 1996; Genever et al., 1999; Kirkpatrick et al., 2001; Zhang et al., 2002], and is typically associated with catalytic activity.

AChE is a single enzyme encoded by a single gene although several isoforms exist due to variable splicing of exons. AChE is assembled into monomers, dimers, and tetramers that may exist as soluble forms in the cytoplasm. Dimers and tetramers may be attached to the plasma membrane via a glycophosphatidylinositol anchor. More complex "asymmetric" isoforms are made up of multiple tetramers tethered by a collagen tail. Most isoforms are found in the central and peripheral nervous systems [Taylor and Radic, 1994; Soreq and Seidman, 2001]. Isoforms have also been characterized in hematopoietic cells, as well as in tumor cells [Karpel et al., 1994; Nechushtan et al., 1996; Perry et al., 2002]. The different isoforms have been shown by reverse-transcriptase polymerase chain reaction (RT-PCR) to result from alternative splicing of AChE mRNA leading to isoforms of AChE protein differing in their 3′ exon composition [Karpel et al., 1994; Perry et al., 2002]. Although long thought that the transcriptional processing of AChE is complex and cell-regulated, additional isoforms continue to be demonstrated [Meshorer et al., 2004].

A hallmark of AChE is its catalytic activity. The presence or absence of AChE in tissues or cells is typically determined by a spectrophotometric enzymatic hydrolysis rate assay called the Ellman assay [Ellman et al., 1961]. The Ellman assay is sensitive, rapid, and capable of measuring very low amounts of AChE catalytic activity. Neuronal cell lines and tissues are routinely assayed for ACh hydrolysis activity by the Ellman assay, but generally, tissue and cell lines that show negligible activity are considered negative for AChE protein expression [Kronman et al., 1992; Kris et al., 1994; Zhang et al., 2002].

Due to the complex assembly and functions of AChE in diverse cell types, we hypothesized that the common correlation of AChE-specific catalytic activity and AChE protein expression levels may be inaccurate, and that the localization of AChE within the cell types may be indicative of catalytic activity. Cellular localization effects on the function of enzymes is a well-studied phenomenon in cell biology, particularly signal transduction factors and transcription factors (reviewed by [Ko and Prives, 1996; Boonstra and Verkleij, 2004]), and we hypothesized that due to the complex assembly of AChE, the cellular location of the enzyme may have a relevant effect on its catalytic activity. Catalytic activity was compared between a panel of primary and immortal cells, and between neuronal and non-neuronal cells. mRNA and protein expression was also compared. There was not a clear correlation between AChE-specific catalytic activity and protein expression. All cell types examined expressed similar amounts of protein, yet very different amounts of catalytic activity. Immunofluorescence and confocal microscopy demonstrated that the cellular localization of AChE was different between neuronal and non-neuronal cells.

MATERIALS AND METHODS

Cell Line Culture

All cell lines were cultured in the recommended media (American Type Cell Culture (ATCC), Manassas, VA), including fetal bovine serum (FBS) and antibiotics. SH-SY5Y human neuroblastoma cells and HeLa human epithelial cells were purchased (ATCC). LLC-MK2 monkey kidney cells, THP-1 acute monocytic leukemia cells, and PC-12 adrenal chromaffin cells were generously provided by Dr. Keith Parker, Dr. Elizabeth Putnam, and Dr. Fernando Cardozo-Pelaez (all of The University of Montana), respectively. PC-12 cells were grown on poly-L-lysine-coated coverslips, and treated with nerve growth factor (NGF, Sigma-Aldrich, St. Louis, MO) at a final concentration of 100 ng/ml or vehicle (phosphate-buffered saline, PBS) for 5 days before analysis.

Primary Cell Culture

Primary rat cerebellar granule neurons (CGN) were isolated from 7-day-old rat pups as described [Schousboe et al., 1989]. The tissue was minced and cells were dissociated with 0.025% trypsin for 15 min at 37°C. Cells were plated on glass coverslips coated with poly-L-lysine and maintained in modified Eagle's medium with 24.5 mM KCl, 30 mM glucose, 7 μM para-aminobenzoic acid, 100 mU/L insulin, and

10% FBS. Twenty four hours after plating, cells were treated with 20 μM cytosine arabinoside to inhibit the growth of non-neuronal cells. Cells were stained for immunofluorescence on day 8 in vitro. Astrocyte Type I cultures were isolated from 3-day-old rats as described [McCarthy and de Vellis, 1980]. Cerebral cortices were harvested and plated in modified Eagle's medium/F12 plus 15% FBS. Twenty-four hours after plating, medium was changed to include 10% FBS. On day 8 in vitro, non-astroycytic cells were removed by shaking the culture overnight. Cultures were relatively pure astrocyte Type I cells, being >95% of glial fibrillary acidic protein-positive cells. Cells were plated onto coverslips on day 13 in vitro for immunofluorescence. Primary human fibroblasts were obtained by mincing foreskin samples from circumcisions and plated in modified Eagle's medium plus 10% FBS (St. Patrick's Hospital and Health Sciences Center, Missoula, MT).

Ellman Assays

Total cellular proteins were harvested from cells by lysis (150 mM NaCl, 1% Triton X-100, 50 mM Tris pH 8.0). Ellman assays were based on published reports, and were performed by incubation of crude protein lysates with 5,5-dithiobis(2-nitrobenzoic acid) (final concentration, 0.32 mM in 0.1M potassium phosphate buffer, pH 7.6) and initiated with acetylthiocholine iodide (ATCh-I) (final concentration, 0.75 mM) [Ellman et al., 1961; George et al., 2001]. BW284c51, an AChE-specific inhibitor or tetraisopropyl pyrophosphoramide (iso-OMPA), a butyrylcholinesterase (BuChE)-specific inhibitor were added (final concentrations, 0.01 mM) 60 min before ATCh-I initiation. Changes in absorbance were measured OD 412 nm at 25°C on a VersaMax microplate reader with Softmax Pro V. 3.0 software. The optimum lengths of time for incubations were determined empirically to allow maximum changes in absorbance for samples versus blanks. Recombinant mouse AChE (rMoAChE) and horse BuChE (hoBuChE, Sigma-Aldrich) were assayed as controls for the inhibitors (data not shown). Ellman assays were performed in triplicate. Statistical analysis was performed with Prism 4.0 software.

Immunoblot Analysis of AChE

Approximately 1×10^7 cells were scraped and proteins extracted in lysis buffer (same as above). Forty micrograms of crude protein lysates were electrophoresed on a 10% SDS–PAGE gel for immunoblot analysis. Primary anti-huAChE monoclonal antibody (Clone 46, BD Biosciences, Mississauga, ON) has previously been used to detect AChE in immunoblot, immunohistochemical, and immunocytochemical assays [Boudreau-Lariviere and Jasmin, 1999; Meshorer et al., 2002; Inkson et al., 2004]. Anti-huAChE was diluted 1:1,500 in blocking buffer (5% non-fat dehydrated milk in PBS/0.3% Tween-20) and secondary anti-mouse IgG conjugated to HRP (Cell Signaling Technology, Beverly, MA) was diluted 1:1,000 in blocking buffer. Primary anti-AChE core polyclonal antibody (N19; Santa Cruz Biotechnologies, Inc., Santa Cruz, CA) has previously been used to detect AChE in immunoprecipitation and immunoblot assays [Birikh et al., 2003; Darreh-Shori et al., 2004; Meshorer et al., 2004]. N19 was diluted 1:500 in blocking buffer, and secondary anti-goat IgG conjugated to HRP (Vector Laboratories, Inc., Burlingame, CA) was diluted 1:2,000 in blocking buffer. For peptide blocking control, the N19 peptide immunogen supplied by the manufacturer was incubated with the N19 antisera at a 10× molar ratio overnight at 4°C in a total volume of 100 μl PBS. The antisera-peptide complexes were ultracentrifuged at 25,000*g* 30 min at 4°C, and supernatant used for hybridization. Immunoblots were detected with an ECL Plus kit (Amersham Biosciences, Piscataway, NJ). Bands were visualized on a VersaDoc imager Model 3000 with Quantity One software (BioRad Laboratories, Hercules, CA).

RT-PCR Primers and Methods

RNA was extracted from 10^7 cells using the RNeasy kit (Qiagen, Valencia, CA). Two micrograms of total RNA was used to transcribe cDNA with Moloney murine leukemia virus reverse transcriptase, random hexamers, RNasin, and dNTP's per manufacturer's instructions (Promega, Madison, WI). Primers for human AChE were:

Exon 1d forward (E1df): 5′-CCTGGTGACGAAAGTCCGA-3′ [Meshorer et al., 2004]
Exon 1d reverse (E1dr): 5′-TCCTCCACCCAGGAGCCAGAG-3′ [Meshorer et al., 2004]
Exon 3 forward (E3f): 5′-CGGGTCTACGCCTACGTCTTTGAACACCGTGCTTC-3′ [Karpel et al., 1994]

Exon 5 reverse (E5r): 5′-TCACAGCCGCCGGAGGTGGGAG-3′
Exon 6 reverse (E6r): 5′-CACAGGTCTGAGCAGCGATCCTGCTTGCTG-3′ [Karpel et al., 1994].

PCR was performed with the following combinations of primers: E1df/E1dr were used to amplify the E1d splice variant, and were expected to yield a product of 250 bp. E3f/E5r were used to amplify the E4/E5 splice variant and were expected to yield a product of 492 bp. E3f/E6r were used to amplify the E4/E6 splice variant and were expected to yield a product of 481 bp. β-actin primers were used to amplify actin as an internal control (Maxim Biotech, Inc., South San Francisco, CA) and were expected to yield a product of 303 bp. pGS-AChE, a plasmid containing the cDNA encoding the human AChE cDNA E4/E6 splice variant was a gift from Dr. Oksana Lockridge (University of Nebraska Medical School, Omaha, NE). PCR was performed on 5 μl of cDNA and PCR conditions were as described previously [Karpel et al., 1994; Meshorer et al., 2004]. For E1d, denaturation 94°C 1min; annealing 60°C 1 min; synthesis 72°C 1 min × 39 cycles. For E4/E5 and E4/E6, denaturation 94°C 1 min; annealing 65°C 1 min; synthesis 72°C 1 min × 39 cycles. Amplification products were electrophoresed on a 1.5% agarose gel and stained with 10 μM ethidium bromide. This experiment was performed at least three times with freshly prepared RNA.

Immunofluorescence and Confocal Microscopy Analysis

Cell lines were plated on coverslips in 12-well plates at 1×10^5/well and allowed to adhere for 48 h. Coverslips were processed for immunofluorescence by fixation in 2% paraformaldehyde in PBS (20 min, RT) and permeabilization in 0.1% Triton X-100 in PBS (20 min, RT). Samples were blocked with 2% BSA in PBS (1 h, RT). Primary anti-huAChE monoclonal antibody was diluted 1:1,500 in block and hybridized (1 h, RT). Secondary anti-mouse IgG Alexa Fluor 488 (Molecular Probes, Eugene, OR) was diluted 1:2,000 and added simultaneously with phalloidin red (Cytoskeleton, Inc., Denver, CO) diluted 1:300. Coverslips were inverted onto microscope slides and confocal images were taken with a BioRad Radiance 2000 Laser Scanning System attached to a Nikon Eclipse TE300 microscope. All images were taken with a 100×-oil objective (with the exception of Fig. 4D, which used a 40× objective), using a double label green/red method (Ar 488 laser and HeNe 543 laser) and the settings were similar for all images. Controls were incubated with secondary antibodies in the absence of primary antibody.

RESULTS

Cell lines and primary cells were chosen for this study to represent a broad range of origin and tissues. SH-SY5Y and HeLa cells are both naturally occurring cancer cell lines. SH-SY5Y cells arose from a thrice-cloned subline of the neuroblastoma, SK-N-SH [Ross et al., 1983]. HeLa cells arose from a cervical carcinoma and are epithelial in nature [Jones et al., 1971]. LLC-MK2 cells are normal monkey kidney cells that are also epithelial in nature [Hull et al., 1962]. THP-1 cells are a human acute monocytic leukemia cell line [Tsuchiya et al., 1980]. CGN and Type I astrocytes were also analyzed to compare primary neuronal and non-neuronal cell types.

AChE-Specific Catalytic Activity in Neuronal and Non-Neuronal Cells

Ellman assays were designed to determine how much total ACh hydrolysis activity the cells express and inhibitors specific for AChE (BW284c51) or BuChE (iso-OMPA) were included to determine the amount of catalytic activity that the specific esterases contribute to the total activity. BuChE is a serine hydrolase that is widely expressed and can react with the ATCh-I substrate and contaminate the Ellman assay [George et al., 2001]. The total amount of Ellman activity in SH-SY5Y was small, but comparable to that reported in other articles (Fig. 1) [Ehrich et al., 1995]. SH-SY5Y cells expressed significantly more total Ellman activity than HeLa and THP-1 cells (Fig. 1, see legend for explanation of symbols). The AChE-specific inhibitor, BW284c51, was used to quantitate the AChE-specific contribution to Ellman activity in cells. By comparing the amount of Ellman activity after BW284c51 treatment with no treatment, a quantitative measurement of AChE-specific catalytic activity can be determined. BW284c51 treatment resulted in reduction of the total amount of Ellman activity in SH-SY5Y cells by 25%,

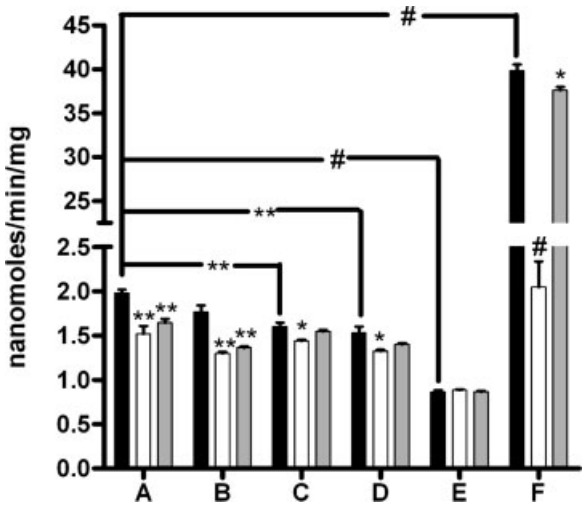

Fig. 1. Ellman assay of ACh hydrolysis activity in cell lines and primary cells. Ellman assays were performed on crude protein lysates either untreated (black bars), or treated with the AChE-specific inhibitor, BW284c51 (white bars), or the BuChE-specific inhibitor, iso-OMPA (gray bars). ACh hydrolysis activity is expressed as nanomoles substrate hydrolyzed/min/mg. (**A**) SH-SY5Y, (**B**) LLC-MK2, (**C**) HeLa, (**D**) THP-1, (**E**) astrocytes, (**F**) cerebellar granule neurons (CGN). Samples were analyzed in triplicate, and the results shown are average activity with standard error of the mean. Statistical analysis was performed to compare the untreated versus treated samples and the SH-SY5Y total Ellman activity (untreated) versus other untreated samples using unpaired, two-tailed *t*-tests (GraphPad Prism v. 4). $^{*} = P < 0.05$; $^{**} = P < 0.01$; $^{\#} = P < 0.0001$.

indicating that there is a significant amount of catalytically active AChE in neuroblastoma cells (Fig. 1). BW284c51 treatment resulted in reduced amounts of Ellman activity in LLC-MK2, HeLa, and THP-1 cells, indicating that these non-cholinergic cell types also express catalytically active AChE. The BuChE-specific inhibitor, iso-OMPA, was used to quantitate the BuChE-specific contribution to Ellman activity. Similar to BW284c51, a quantitative measurement of BuChE-specific catalytic activity can be determined by comparing the amount of Ellman activity after iso-OMPA treatment with no treatment. Iso-OMPA treatment resulted in significantly reduced Ellman activity in SH-SY5Y and LLC-MK2 cells, but not in the HeLa or THP-1 cells. This indicates that BuChE catalytic activity is present in significant amounts in SH-SY5Y and LLC-MK2 cells, but not in HeLa or THP-1 cells (Fig. 1). The remaining Ellman activity that was not inhibited by BW284c51 or iso-OMPA is presumably due to other contaminating esterases present in these cells.

Primary astrocytes and CGN were analyzed similarly. CGN expressed ~20 fold more Ellman activity than the SH-SY5Y cells. BW284c51 treatment of CGN inhibited total Ellman activity by 96%, indicating that AChE contributed to the majority of Ellman activity in these cells. Iso-OMPA treatment of CGN also reduced the Ellman activity, indicating BuChE expression in these cells. Astrocytes expressed the least amount of Ellman activity of any cell type tested, and was not changed by either treatment. ACh hydrolysis activity in primary human fibroblasts was also analyzed by the Ellman assay. BW284c51 treatment had no significant effect on Ellman activity in primary human fibroblasts, but iso-OMPA treatment resulted in a significant reduction in Ellman activity (data not shown).

Several trends emerged from this experiment; firstly, neurons expressed more AChE-specific catalytic activity than non-neuronal cells, and secondly, the primary neurons (CGN) expressed much more AChE-specific activity than the SH-SY5Y neuroblastoma cell line. All primary cells and cell lines tested, with the exception of astrocytes, expressed AChE-specific activity, and the SH-SY5Y, LLC-MK2, and the CGN expressed BuChE-specific activity, while the HeLa and THP-1 cells did not.

Protein Analysis of AChE

To correlate the amount of AChE-specific catalytic activity with the amount of protein expressed, cell lines were analyzed for AChE protein by immunoblot. Equal amounts of crude protein lysates were analyzed for AChE protein by hybridization with a commercially available anti-human AChE monoclonal antibody (anti-huAChE) raised against a large immunogen that encompasses the last 200 amino acids of the E4/E6 isoform of AChE (Fig. 2A, top panel), as well as a commercially available polyclonal anti-AChE antibody (N19) that was raised against a peptide corresponding to the N-terminus of AChE (Fig. 2A, middle panel). The anti-huAChE antibody recognized a single band that migrated at the approximate mass for AChE protein, 65 kDa. This band was detected by the antibody at similar levels in all four cell lines and primary cells. The N19 antibody recognized a band in all lysates that migrated at the same position as the band that anti-huAChE antibody recognized (Fig. 2A, middle panel). In contrast to anti-huAChE, the levels of

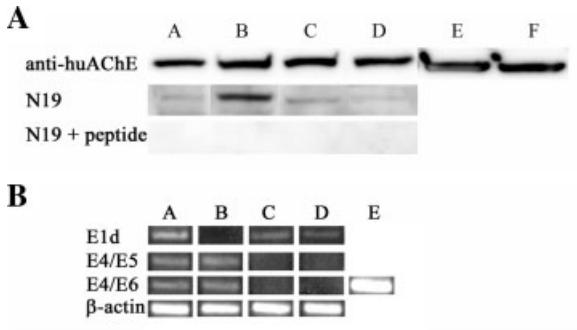

Fig. 2. Expression of AChE protein and transcript in cell lines. (**A**) Immunoblot analysis of AChE expression in cell lines. Equivalent (μg) amounts of crude protein lysates were analyzed, and the band detected by the antibody migrated at approximately 65 kDa. **Top panel**, Anti-huAChE antibody; **Middle panel**, N19 antibody; **Bottom panel**, N19 antibody pre-adsorbed with N19 peptide. **Lane A**, SH-SY5Y; **lane B**, LLC-MK2; **lane C**, HeLa; **lane D**, THP-1, **lane E**, astrocytes, **lane F**, CGNs. **B**: RT-PCR analysis of AChE splice variants E1d, E4/E5, E4/E6, and β-actin. **Lane A**, SH-SY5Y, **lane B** LLC-MK2, **lane C** HeLa, and **lane D** THP-1. **Lane E**, pGS-AChE cDNA was used as positive control for the E4/E6 variant. Primers, sizes of expected products, and RT-PCR conditions were as described in Materials and Methods.

AChE detected by N19 varied in different cell lysates. The LLC-MK2 cells expressed the highest amount of the form of AChE recognized by N19 (Fig. 2A, middle panel, lane B). To confirm the specificity of the N19 antibody, the antisera was preadsorbed with the peptide antigen of N19 (Fig. 2A, bottom panel). Pre-adsorption of N19 with its peptide antigen completely blocked reactivity with the AChE band that co-migrates with both antibodies, confirming that the protein recognized by both antibodies is AChE.

Transcript Analysis of AChE

The two antibodies used in the immunoblot were raised against different portions of AChE, and the relative levels of protein detected by the two antibodies differed. Therefore, it was of interest to determine which AChE mRNA splice variants could be detected by RT-PCR. In mammals, all AChE transcripts contain exon 1, 2, 3, and 4 (E4), but exon 5 (E5) and exon 6 (E6) are variably spliced onto the 3′ end of the mRNA. The variant that contains E5 is termed E4/E5 and is expressed in erythroid cells and tumor cells. The variant that contains E6 is termed E4/E6, and is expressed in neuronal tissue. Recently, a novel alternative exon 1 (E1d) has been identified in the human *AChE* gene, and was shown to be expressed in neuronal tissue and leukocytes [Meshorer et al., 2004]. All three splice variants were detected in SH-SY5Y cells (Fig. 2B, lane A). The E4/E5 and E4/E6 splice variants were detected in LLC-MK2 cells; however, the E1d variant was not (Fig. 2B, lane B). The E1d variant was detected in HeLa and THP-1 cells, however neither the E4/E5 nor the E4/E6 splice variant was detected (Fig. 2B, lane C and D) (Fig. 2B, lane D). The expression of the E1d variant in THP-1 cells is consistent with that variant being expressed in leukocytes [Meshorer et al., 2004]. The internal control primers for actin showed that equivalent amounts of cDNA were present in each sample (Fig. 2B). pGS-AChE, a plasmid containing the cDNA encoding the E4/E6 splice variant, was used as a positive control for amplification of the E4E6 variant (Fig. 2B, lane E). This experiment was performed at least three times with freshly prepared RNA, with identical results.

AChE Localization in Cell Lines

The result that neuronal and non-neuronal cells express equivalent levels of AChE protein, yet non-equivalent levels of catalytically active AChE, led us to hypothesize that the protein localization may be different between neuronal cells and non-neuronal cells. The localization pattern of AChE was analyzed by confocal microscopy by hybridization with the anti-huAChE monoclonal antibody and counter-stained with phalloidin red to stain f-actin. Phalloidin staining allowed visualization of the total cell body, and in particular, all neurite extensions. In SH-SY5Y cells, AChE protein had a diffuse distribution in the cytoplasm, and a punctate pattern on the neurites (Fig. 3A,B).

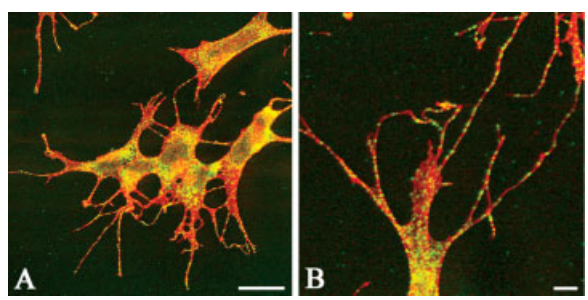

Fig. 3. Confocal microscopy image of AChE localization in SH-SY5Y cells. (**A**) Confocal image of SH-SY5Y cells stained for AChE (green) and actin (red) as described in Materials and Methods. (**B**) Higher magnification of AChE staining in SH-SY5Y cells highlighting punctate staining on neurites that extend between cells. Scale bars = 20 μm.

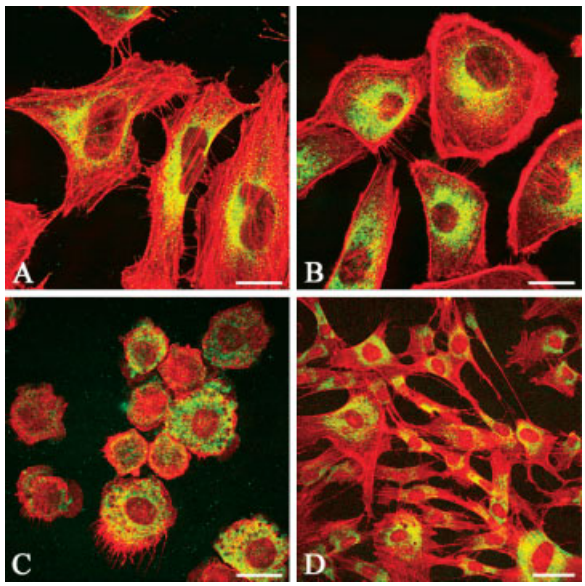

Fig. 4. Confocal microscopy image of AChE staining in non-neuronal cells. Cells were processed as in Figure 3 and stained for AChE (green) and actin (red). (**A**) HeLa cells, (**B**) LLC-MK2 cells, (**C**) THP-1 cells, and (**D**) primary human fibroblasts. Scale bars (A–C) = 20 μm. Scale bar (D) = 50 μm.

Subsequently, the non-neuronal cells, HeLa, LLC-MK2, THP-1 cells, and primary human fibroblasts were stained for AChE and actin. In all non-neuronal cells, AChE protein was present in high amounts in the cytoplasm (Fig. 4A–D). AChE was clearly not expressed on the cell surface, as compared to the phalloidin staining that labels the cell body out to the plasma membrane. AChE expression in the cytoplasm was different between the neuroblastomas and non-neuronal cells. In non-neuronal cells, the staining was very intense in the perinuclear region, while in neuroblastomas the staining was diffuse throughout the cytoplasm.

As a further examination of AChE localization in neuronal cells, rat primary CGN and primary astrocyte Type I cultures were analyzed for AChE expression by confocal microscopy. AChE localization in CGN closely approximated the pattern in the SH-SY5Y neuroblastoma cells. Staining was diffuse throughout the cytoplasm and punctate along the neurites (Fig. 5A). The AChE localization pattern in the astrocyte Type I cells was essentially the same as for all other non-neuronal cells examined (Fig. 5B). Staining was intensely localized in the perinuclear region and no staining was apparent along the plasma membrane.

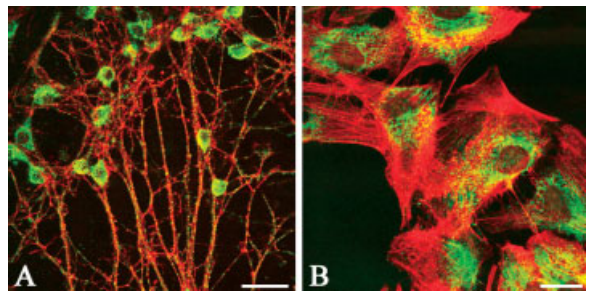

Fig. 5. Confocal microscopy image of AChE staining in primary cell cultures. Cells were processed as in Figure 3 and stained for AChE (green) and actin (red). (**A**) CGN, (**B**) Type I astrocytes. Scale bars = 20 μm.

AChE Localization Changes in PC-12 Cells Following NGF-Induced Differentiation

The localization of AChE was different between neuronal and non-neuronal cells, therefore, it was of interest to analyze the localization in a cell type that is non-neuronal in nature, but can be induced to differentiate as neuronal. PC-12 cells are an excellent model system to answer the question whether AChE localization is truly different between non-neuronal and neuronal cells as undifferentiated PC-12 cells are round, adrenal chromaffin cells. After NGF treatment, PC-12 differentiate to resemble sympathetic neurons, extend neurites, slow down in proliferation, and express 2–4 fold more AChE catalytic activity, as well as other neuronal markers [Lucas and Kreutzberg, 1985; Shafer and Atchison, 1991]. Localization of AChE in undifferentiated and differentiated PC-12 cells was analyzed by confocal microscopy. Undifferentiated PC-12 cells expressed AChE and its localization was similar to other non-neuronal cells analyzed (Fig. 6A,B), with the majority of staining in the perinuclear region. AChE was not present on the plasma membrane when compared to the phalloidin staining. Upon NGF-treatment (100 ng/ml, 5 days), the localization of AChE changed to a neuronal-like staining pattern (Fig. 6C,D). AChE was expressed along the neurites, whilst the cytoplasmic staining was augmented and expanded to encompass the whole cell, as compared to the undifferentiated PC-12 cells. This staining pattern is consistent with reports of localization of AChE catalytic activity in NGF-treated PC-12 cells [Schweitzer, 1993]. The intensity of the AChE staining also increased after NGF-treatment, consistent with an increase in production of enzyme upon differentiation. The different

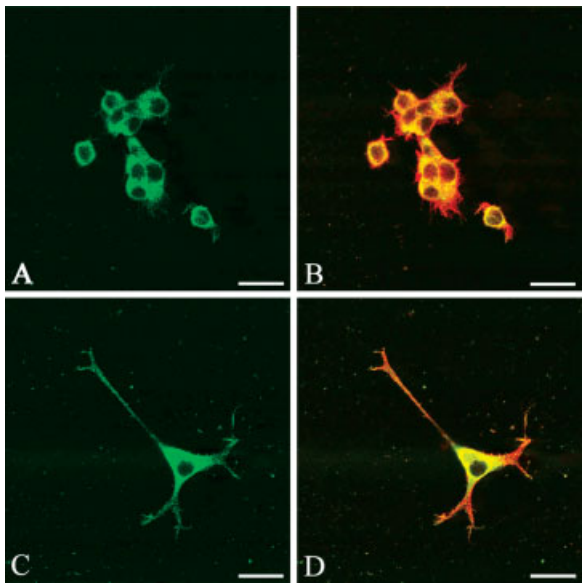

Fig. 6. Confocal microscopy image of AChE staining in undifferentiated and NGF-differentiated PC-12 cells. PC-12 cells were stained for AChE immunofluorescence. (**A**, **B**) Undifferentiated PC-12 cells, (**C**, **D**) PC-12 treated with 100 ng/ml NGF for 5 days. (A) and (C); AChE (green) staining. (B) and (D); the merge of AChE (green) and actin (red) staining. Scale bars = 20 μm.

localization of AChE in PC-12 cells before and after NGF treatment elegantly demonstrated that AChE localization changes during neuronal differentiation.

DISCUSSION

This study compared biochemical parameters of AChE expression between neuronal and non-neuronal cells, and the potential role of protein localization with protein function. The data is summarized in Table I. Neuronal cells expressed more AChE-specific catalytic activity than non-neuronal cells, while the primary CGN expressed ~20-fold more AChE-specific activity than the neuroblastoma cell line. By immunoblot, AChE protein was detected in all cell types examined, but the levels of AChE protein detected differed depending on which of two commercially available anti-AChE antibodies was used. To confirm the immunoblot results, AChE mRNA splice variants were amplified by RT-PCR. All cell lines expressed at least one splice variant. Further examination of AChE by confocal microscopy revealed two patterns of AChE localization that can be classified as "neuronal" or "non-neuronal". The neuronal pattern consisted of diffuse cytoplasmic staining and plasma membrane- and neurite-associated punctate staining, while the non-neuronal pattern consisted of intense perinuclear staining with no staining on the plasma membrane. Together this data suggests the hypothesis that AChE catalytic activity may not be correlated with protein expression, as all cell lines examined expressed similar levels of AChE protein, yet displayed a wide range of AChE catalytic activity that may be correlated with protein localization.

A significant result of this study was the finding that regardless of the amount of AChE-specific catalytic activity, most cell lines expressed the AChE protein by immunoblot and immunofluorescence analysis, and that the localization was different between neuronal and non-neuronal cells. To confirm the immunoblot analysis, two commercially available anti-AChE antibodies that recognize different regions of AChE were utilized, and both detected a band

TABLE I. Evidence for AChE Expression in Different Cell Types

		mRNA			Protein		
	AChE activity	E1d	E4/E5	E4/E6	Anti-huAChE	N19	Localization
SH-SY5Y	++	+	+	+	+++	++	Neuronal
LLC-MK2	++	−	+	+	+++	+++	Non-neuronal
HeLa	+	+	−	−	+++	++	Non-neuronal
THP-1	+	+	−	−	+++	++	Non-neuronal
Astrocytes	−	n.d.	n.d.	n.d.	+++	n.d.	Non-neuronal
CGN	++++	n.d.	n.d.	+[a]	+++	n.d.	Neuronal
PC-12	Yes[b]	n.d.	+[c]	+[c]	n.d.	n.d.	Non-neuronal
PC-12/NGF	Yes[b]	n.d.	n.d.	n.d.	n.d.	n.d.	Neuronal
Primary human fibroblasts	−[d]	n.d.	n.d.	n.d.	++[d]	n.d.	Non-neuronal

Summary from data presented here and in other reports.
n.d., not determined.
[a]Meshorer et al. [2002].
[b]Lucas and Kreutzberg [1985].
[c]Grifman and Soreq [1997].
[d]data not shown.

that migrated at the same position, and corresponds to the molecular weight of AChE. However, the levels and quality of detection of AChE were very different for the two antibodies. The monoclonal anti-huAChE antibody that has been utilized for cytochemical analyses of AChE in other studies (see Introduction) recognized a single band and the density of the band was similar in all cell lines and cell types examined. The relatively equivalent abundance of AChE recognized by the anti-huAChE antibody was confirmed by immunofluorescence analysis that showed similar levels of AChE fluorescence with that same antibody. N19 is a polyclonal antibody raised against a peptide that corresponds to the N-terminus, and immunoblots hybridized with N19 exhibited more background bands, although the predominant band migrated at the same position as the band recognized by anti-huAChE antibody. Additionally, the density of the AChE band recognized by N19 was different between all the cell lines, indicating different amounts of AChE proteins. This may be due to different qualities of the two antibodies, or to the abundance of different isoforms of AChE expressed that the antibodies differentially recognize.

In order to preliminarily characterize the structure of the AChE expressed in cell lines, AChE mRNA was analyzed in the cell lines. In mammals, all AChE transcripts contain exon 1, 2, 3, and 4 (E4), and exhibit variable splicing on the 5′ and 3′ ends. Exon 5 (E5) and exon 6 (E6) are variably spliced onto the 3′ end of the mRNA. An alternative exon 1 (E1d) has recently been shown to be variably spliced onto the 5′ end of human AChE [Meshorer et al., 2004], and results in a protein that migrated at a slightly higher molecular weight by immunoblot with an antibody specific to E1d. RT-PCR analysis of the cell lines demonstrated a complex array of splice variant types. While SH-SY5Y, HeLa, and THP-1 cells expressed the E1d variant, the protein detected by anti-huAChE or N19 antibodies migrated identically on SDS–PAGE (Fig. 2A). Since the HeLa and THP-1 cells did not amplify with either set of 3′ primers, it is not clear as to the content of the 3′ end of those transcripts or the protein identified on immunoblot. The immunogen, to which the anti-huAChE monoclonal antibody was raised against, according to the manufacturer, corresponds to amino acids 411–609 of human AChE. Although the exact epitope of the monoclonal antibody is not known, the total immunogen encompassed half of exon 3, all of exon 4, and most of exon 6. The possibility exists that other, as yet unidentified, splice variants exist in these cell types.

Comparing the neuroblastomas to CGNs revealed many similarities in protein levels and localization, but a discrepancy in the levels of AChE catalytic activity. All neuronal cell types, SH-SY5Y, NGF-stimulated PC-12 cells, and CGN exhibited a similar localization pattern. The localization of AChE in neuronal cells is supported in data from other laboratories that analyzed the localization of AChE catalytic activity by histochemical methods [Spencer and Baker, 1986; Tago et al., 1986; Greenfield, 1991; Anglade et al., 1999], immunocytochemical data [Rotundo and Carbonetto, 1987; Tojima et al., 2000], and flow cytometry [Pick et al., 2004]. While the neuronal localization pattern was identical, the primary CGN expressed ~20-fold more AChE catalytic activity than the SH-SY5Y cell line. This may be due in part to the fact that SH-SY5Y are tumor cells, which may possess genomic or cellular changes that interact with AChE inhibit its catalytic activity. It was also surprising that CGN express such a high level of catalytic activity and protein, because CGN are primarily glutamatergic, however express cholinergic receptors, but have not previously been shown to express high levels of AChE [Schousboe et al., 1985; Fucile et al., 2004]. AChE has been shown to be involved transiently in neuritogenesis, and the CGN may represent immature neurons that express AChE prior to other more mature glutamatergic markers [Layer, 1990; Dong et al., 2004].

AChE is generally considered catalytically active when expressed; however, the presence of inactive and active AChE in cells has been demonstrated in the chicken. AChE antibodies have been raised against chicken brain AChE that differentially recognized catalytically active or total AChE [Chatel et al., 1993]. From comparison of enzyme bound by each antibody, the amount of catalytically inactive AChE was estimated to be 30% of total. Another group used anti-AChE antibodies raised against chicken brain AChE that recognized total AChE [Rotundo, 1988]. By comparing isotopically labeled enzyme (that had been immunoprecipitated) with catalytically active enzyme, it was concluded that a large proportion of newly synthesized AChE (70%–80%) was rapidly degraded in the endoplasmic reticulum (ER).

Both of these studies examined AChE in brain tissue, but they raise the possibility that non-catalytically active AChE may be expressed in some cell types. It may be that AChE in non-neuronal cells is sequestered in the ER as a non-catalytically active form that requires glycosylation for catalytic activity.

Due to amino acid sequence homology of AChE with cell adhesion proteins, such as gliotactin, glutactin, and neuroligins, AChE has been shown capable of promoting cellular adhesion of neurons and osteoblasts [Inkson et al., 2004; Johnson and Moore, 2004]. AChE may promote adhesion of epithelial cell lines, such as HeLa and LLC-MK2 cells, however, this study showed AChE is localized to the perinuclear region of these cells, and not on the plasma membrane, indicating involvement of other cellular factors in adhesion of these types of cell. AChE has been shown to exhibit aryl acylamidase activity during chicken brain development [Checler et al., 1994; Boopathy and Layer, 2004]. This amidase activity paralleled the catalytic activity of AChE during development. While these alternative functions have been demonstrated, the localization of AChE within the cell types examined was not analyzed.

These results lead to the conclusion that, although AChE protein is expressed in most cell types, its localization with respect to catalytic activity in neuronal versus non-neuronal cells is very different. This change in localization may play some role in the function of AChE, and possibly catalytic activity of the enzyme. In summary, AChE expression is more complex than traditionally thought, and cannot be correlated with catalytic activity, but is regulated through cellular localization in neuronal and non-neuronal cell types.

ACKNOWLEDGMENTS

The authors thank Carla Burgess, Sarjubhai Patel, David Walker, and Todd Struckman for technical advice and support. The content of the information in this report does not necessarily reflect the position or the policy of the US Army or Department of Defense, and no official endorsement should be inferred.

REFERENCES

Anglade P, Grassi J, Motelica-Heino I, Hashikawa T, Tsuji S. 1999. Ultrastructural evidence for dendritic release of acetylcholinesterase in the rat substantia nigra. Folia Histochem Cytobiol 37:243–247.

Birikh KR, Sklan EH, Shoham S, Soreq H. 2003. Interaction of "readthrough" acetylcholinesterase with RACK1 and PKCbeta II correlates with intensified fear-induced conflict behavior. Proc Natl Acad Sci USA 100:283–288.

Boonstra J, Verkleij AJ. 2004. Regulation of enzyme activity in vivo is determined by its cellular localization. Adv Enzyme Regul 44:61–73.

Boopathy R, Layer P. 2004. Aryl acylamidase activity on acetylcholinesterase is high during early chicken brain development. Protein J 23:325.

Boudreau-Lariviere C, Jasmin BJ. 1999. Calcitonin gene-related peptide decreases expression of acetylcholinesterase in mammalian myotubes. FEBS Lett 444:22–26.

Chatel JM, Grassi J, Frobert Y, Massoulie J, Vallette FM. 1993. Existence of an inactive pool of acetylcholinesterase in chicken brain. Proc Natl Acad Sci USA 90:2476–2480.

Checler F, Grassi J, Vincent JP. 1994. Cholinesterases display genuine arylacylamidase activity but are totally devoid of intrinsic peptidase activities. J Neurochem 62: 756–763.

Darreh-Shori T, Hellstrom-Lindahl E, Flores-Flores C, Guan ZZ, Soreq H, Nordberg A. 2004. Long-lasting acetylcholinesterase splice variations in anticholinesterase-treated Alzheimer's disease patients. J Neurochem 88:1102–1113.

Day T, Greenfield SA. 2002. A non-cholinergic, trophic action of acetylcholinesterase on hippocampal neurones in vitro: Molecular mechanisms. Neuroscience 111:649–656.

Dong H, Xiang YY, Farchi N, Ju W, Wu Y, Chen L, Wang Y, Hochner B, Yang B, Soreq H, Lu WY. 2004. Excessive expression of acetylcholinesterase impairs glutamatergic synaptogenesis in hippocampal neurons. J Neurosci 24: 8950–8960.

Ehrich M, Correll L, Carlson K, Wilcke J, Veronesi B. 1995. Examination of culture conditions on esterase activities in human and mouse neuroblastoma cell lines. In Vitr Toxicol 8:199–206.

Ellman GL, Courtney KD, Andres V, Jr., Featherstone RM. 1961. A new and rapid colorimetric determination of acetylcholinesterase activity. Biochem Pharmacol 7:88–95.

Fucile S, Renzi M, Lauro C, Limatola C, Ciotti T, Eusebi F. 2004. Nicotinic cholinergic stimulation promotes survival and reduces motility of cultured rat cerebellar granule cells. Neuroscience 127:53–61.

Genever PG, Birch MA, Brown E, Skerry TM. 1999. Osteoblast-derived acetylcholinesterase: A novel mediator of cell- matrix interactions in bone? Bone 24:297–303.

George KM, Montgomery MA, Sandoval LE, Thompson CM. 2001. Examination of cross-antigenicity of acetylcholinesterase and butyrylcholinesterase using anti-acetylcholinesterase antibodies. Toxicol Lett 126:99–105.

Greenfield SA. 1991. A noncholinergic action of acetylcholinesterase (AChE) in the brain: From neuronal secretion to the generation of movement. Cell Mol Neurobiol 11: 55–77.

Grifman M, Soreq H. 1997. Differentiation intensifies the susceptibility of pheochromocytoma cells to antisense oligodeoxynucleotide-dependent suppression of acetyl-

cholinesterase activity. Antisense Nucleic Acid Drug Dev 7:351–359.
Grisaru D, Sternfeld M, Eldor A, Glick D, Soreq H. 1999. Structural roles of acetylcholinesterase variants in biology and pathology. Eur J Biochem 264:672–686.
Hull RN, Cherry WR, Tritch OJ. 1962. Growth characteristics of monkey kidney cell strains LLC-MK1, LLC-MK2, and LLC-MK2(NCTC-3196) and their utility in virus research. J Exp Med 115:903–918.
Inestrosa NC, Alvarez A, Perez CA, Moreno RD, Vicente M, Linker C, Casanueva OI, Soto C, Garrido J. 1996. Acetylcholinesterase accelerates assembly of amyloid-beta-peptides into Alzheimer's fibrils: Possible role of the peripheral site of the enzyme. Neuron 16:881–891.
Inkson CA, Brabbs AC, Grewal TS, Skerry TM, Genever PG. 2004. Characterization of acetylcholinesterase expression and secretion during osteoblast differentiation. Bone 35:819–827.
Johnson G, Moore SW. 2004. Identification of a structural site on acetylcholinesterase that promotes neurite outgrowth and binds laminin-1 and collagen IV. Biochem Biophys Res Commun 319:448–455.
Jones HW, Jr., McKusick VA, Harper PS, Wuu KD. 1971. George Otto Gey. (1899–1970). The HeLa cell and a reappraisal of its origin. Obstet Gynecol 38:945–949.
Karpel R, Ben Aziz-Aloya R, Sternfeld M, Ehrlich G, Ginzberg D, Tarroni P, Clementi F, Zakut H, Soreq H. 1994. Expression of three alternative acetylcholinesterase messenger RNAs in human tumor cell lines of different tissue origins. Exp Cell Res 210:268–277.
Karpel R, Sternfeld M, Ginzberg D, Guhl E, Graessmann A, Soreq H. 1996. Overexpression of alternative human acetylcholinesterase forms modulates process extensions in cultured glioma cells. J Neurochem 66:114–123.
Kirkpatrick CJ, Bittinger F, Unger RE, Kriegsmann J, Kilbinger H, Wessler I. 2001. The non-neuronal cholinergic system in the endothelium: Evidence and possible pathobiological significance. Jpn J Pharmacol 85:24–28.
Ko LJ, Prives C. 1996. p53: Puzzle and paradigm. Genes Dev 10:1054–1072.
Koenigsberger C, Chiappa S, Brimijoin S. 1997. Neurite differentiation is modulated in neuroblastoma cells engineered for altered acetylcholinesterase expression. J Neurochem 69:1389–1397.
Kris M, Jbilo O, Bartels CF, Masson P, Rhode S, Lockridge O. 1994. Endogenous butyrylcholinesterase in SV40 transformed cell lines: COS-1, COS-7, MRC-5 SV40, and WI-38 VA13. In Vitro Cell Dev Biol Anim 30A:680–689.
Kronman C, Velan B, Gozes Y, Leitner M, Flashner Y, Lazar A, Marcus D, Sery T, Papier Y, Grosfeld H, et al. 1992. Production and secretion of high levels of recombinant human acetylcholinesterase in cultured cell lines: Microheterogeneity of the catalytic subunit. Gene 121: 295–304.
Lan CT, Shieh JY, Wen CY, Tan CK, Ling EA. 1996. Ultrastructural localization of acetylcholinesterase and choline acetyltransferase in oligodendrocytes, glioblasts and vascular endothelial cells in the external cuneate nucleus of the gerbil. Anat Embryol (Berl) 194:177–185.
Layer PG. 1990. Cholinesterases preceding major tracts in vertebrate neurogenesis. Bioessays 12:415–420.
Lucas CA, Kreutzberg GW. 1985. Regulation of acetylcholinesterase secretion from neuronal cell cultures-1. Actions of nerve growth factor, cytoskeletal inhibitors and tunicamycin. Neuroscience 14:349–360.
McCarthy KD, de Vellis J. 1980. Preparation of separate astroglial and oligodendroglial cell cultures from rat cerebral tissue. J Cell Biol 85:890–902.
Meshorer E, Erb C, Gazit R, Pavlovsky L, Kaufer D, Friedman A, Glick D, Ben-Arie N, Soreq H. 2002. Alternative splicing and neuritic mRNA translocation under long-term neuronal hypersensitivity. Science 295:508–512.
Meshorer E, Toiber D, Zurel D, Sahly I, Dori A, Cagnano E, Schreiber L, Grisaru D, Tronche F, Soreq H. 2004. Combinatorial complexity of 5′ alternative acetylcholinesterase transcripts and protein products. J Biol Chem 279:29740–29751.
Nechushtan H, Soreq H, Kuperstein V, Tshori S, Razin E. 1996. Murine and human mast cell express acetylcholinesterase. FEBS Lett 379:1–6.
Ollis DL, Cheah E, Cygler M, Dijkstra B, Frolow F, Franken SM, Harel M, Remington SJ, Silman I, Schrag J, et al. 1992. The alpha/beta hydrolase fold. Protein Eng 5:197–211.
Perry C, Sklan EH, Birikh K, Shapira M, Trejo L, Eldor A, Soreq H. 2002. Complex regulation of acetylcholinesterase gene expression in human brain tumors. Oncogene 21:8428–8441.
Pick M, Flores-Flores C, Grisaru D, Shochat S, Deutsch V, Soreq H. 2004. Blood-cell-specific acetylcholinesterase splice variations under changing stimuli. Int J Dev Neurosci 22:523–531.
Ross R, Spengler B, Biedler J. 1983. Coordinate morphological and biochemical interconversion of human neuroblastoma cells. J Natl Cancer Inst 71:741–749.
Rotundo RL. 1988. Biogenesis of acetylcholinesterase molecular forms in muscle. Evidence for a rapidly turning over, catalytically inactive precursor pool. J Biol Chem 263:19398–19406.
Rotundo RL, Carbonetto ST. 1987. Neurons segregate clusters of membrane-bound acetylcholinesterase along their neurites. Proc Natl Acad Sci USA 84:2063–2067.
Schousboe A, Drejer J, Hansen GH, Meier E. 1985. Cultured neurons as model systems for biochemical and pharmacological studies on receptors for neurotransmitter amino acids. Dev Neurosci 7:252–262.
Schousboe A, Meier E, Drejer J, Hertz L. 1989. Preparation of primary cultures of mouse (rat) cerebellar granule cells. In Shahar A, de Vellis J, Vernadakis A, Haber B, editors. "A dissection and tissue culture manual of the nervous system." New York: Alan R. Liss, Inc., pp 203–206.
Schweitzer ES. 1993. Regulated and constitutive secretion of distinct molecular forms of acetylcholinesterase from PC12 cells. J Cell Sci 106(Pt 3):731–740.
Shafer TJ, Atchison WD. 1991. Transmitter, ion channel and receptor properties of pheochromocytoma (PC12) cells: A model for neurotoxicological studies. Neurotoxicology 12:473–492.
Soreq H, Seidman S. 2001. Acetylcholinesterase—new roles for an old actor. Nat Rev Neurosci 2:294–302.
Soreq H, Patinkin D, Lev-Lehman E, Grifman M, Ginzberg D, Eckstein F, Zakut H. 1994. Antisense oligonucleotide inhibition of acetylcholinesterase gene expression induces progenitor cell expansion and suppresses hematopoietic apoptosis ex vivo. Proc Natl Acad Sci USA 91: 7907–7911.

Spencer RF, Baker R. 1986. Histochemical localization of acetylcholinesterase in relation to motor neurons and internuclear neurons of the cat abducens nucleus. J Neurocytol 15:137–154.

Tago H, Kumura H, Maeda T. 1986. Visualization of detailed acetylcholinesterase fiber and neuron staining in rat brain by a sensitive histochemical procedure. J Histochem Cytochem 34:1431–1438.

Taylor P, Radic Z. 1994. The cholinesterases: From genes to proteins. Annu Rev Pharmacol Toxicol 34:281–320.

Tojima T, Yamane Y, Takahashi M, Ito E. 2000. Acquistion of neuronal proteins during differentiation of NG108-15 cells. Neurosci Res 37:153–161.

Tsuchiya S, Yamabe M, Yamaguchi Y, Kobayashi Y, Konno T, Tada K. 1980. Establishment and characterization of a human acute monocytic leukemia cell line (THP-1). Int J Cancer 26:171–176.

Whyte KA, Greenfield SA. 2003. Effects of acetylcholinesterase and butyrylcholinesterase on cell survival, neurite outgrowth, and voltage-dependent calcium currents of embryonic ventral mesencephalic neurons. Exp Neurol 184:496–509.

Zhang XJ, Yang L, Zhao Q, Caen JP, He HY, Jin QH, Guo LH, Alemany M, Zhang LY, Shi YF. 2002. Induction of acetylcholinesterase expression during apoptosis in various cell types. Cell Death Differ 9:790–800.